Austrian Journal of Earth Sciences | Volume 98 | 78 - 91 | Vienna | 2005

A Lateglacial travertine deposit in Eastern Tyrol (Austria)

Ronny BOCH[1)*], Christoph SPÖTL[1)], Jürgen M. REITNER[2)] & Jan KRAMERS[3)]

[1)] Institut für Geologie und Paläontologie, Leopold-Franzens-Universität Innsbruck, Innrain 52, 6020 Innsbruck, Austria

[2)] Geologische Bundesanstalt, Neulinggasse 38, 1030 Wien, Austria

[3)] Institut für Geologie, Universität Bern, Erlachstraße 9a, 3012 Bern, Switzerland

[*)] Corresponding author: Ronny Boch (ronny.boch@uibk.ac.at)

KEYWORDS

U-series dating
stable isotopes
Quaternary
lamination
travertine

Abstract

An aragonite-bearing travertine body is preserved on the southwestern flank of the Schober Group near Ainet (Eastern Tyrol, Austria). This occurrence of freshwater carbonates within metamorphic rocks is dated by the U/Th method to 13.5 kyr before present. The deposit overlies ice marginal sediments whose calcite cements predated the onset of travertine deposition by a few hundred years. Aragonite-calcite couplets, typically only about a millimetre thick, constitute the major portion of the ca. 2.5 m thick travertine body and are interpreted as annual layers. An even finer scale lamination of probably diurnal origin is preserved in many aragonite and some calcite layers. The travertine is capped by a thin layer of calcitic tufa. Detailed stable isotope studies suggest a low-temperature origin of the travertine. Aragonite and calcite crystallization occurred at conditions near isotopic equilibrium. No travertine or significant tufa formation occurs in the area today, although streams emerging from small springs are still supersaturated with respect to calcite and to a lesser degree also with regard to aragonite. Their hydrochemical composition is consistent with groundwater intensively interacting with metamorphic rocks in a fractured aquifer. The formation of the travertine body is ultimately linked to a short-lived discharge event of evolved groundwater, probably released along fractures that opened in response to deep-seated gravitational movements (toppling type) on the steep slope facing the Isel Valley.

An der Südwestseite der Schobergruppe nahe Ainet (Osttirol) ist ein Aragonit-führendes Travertinvorkommen aufgeschlossen. Die Uran-Serien-Datierung dieser karbonatischen Süßwasserbildung in kristallinen Gesteinen ergab ein Alter um 13,5 kyr vor heute. Das Vorkommen überlagert Eisrandsedimente, die durch Kalzitzemente verfestigt sind, welche einige hundert Jahre älter sind als der Travertin. Aragonit-Kalzit Couplets, typischerweise einige Millimeter dick, machen den Hauptteil des etwa 2,5 m mächtigen Travertinkörpers aus und werden als jährliche Lagen interpretiert. Eine noch feinere Lamination – wahrscheinlich täglichen Ursprungs – ist in zahlreichen Aragonit- und einigen Kalzitlagen erhalten. Der Travertin wird von geringmächtigem Kalktuff überlagert. Detaillierte Untersuchungen mittels stabiler Isotope sprechen für eine Niedertemperatur-Bildung des Travertins. Die Kristallisation von Aragonit und Kalzit geschah bei Bedingungen nahe dem isotopischen Gleichgewicht. Im Untersuchungsgebiet findet rezent keine Travertin- und keine nennenswerte Quelltuff-Bildung statt, obwohl Oberflächenwässer nach wie vor an Kalzit und in geringerem Maße an Aragonit übersättigt sind. Ihre chemische Zusammensetzung spricht für intensive Interaktion mit Kristallingesteinen in einem stark geklüfteten Aquifer. Die Bildung des Travertins wird mit einem kurzzeitigen Grundwasser-Austritt in Verbindung gebracht. Dieser erfolgte wahrscheinlich entlang von Bewegungsflächen, die durch tiefgreifende Massenbewegungen, im Speziellen Kippungen („toppling"), an diesem steilen Hang des Iseltales bedingt sind.

1. Introduction

Travertine is an important group of freshwater carbonates forming locally extensive terrace-like deposits (Ford and Pedley, 1996; Pentecost, 2005). These deposits are typically well bedded – from outcrop scale down to thin section scale – and exhibit moderate to low primary porosity. Travertine consists of low-Mg calcite or, less abundantly, of aragonite (Guo and Riding, 1992; Fouke et al., 2000). The bulk of the world's travertine deposits appears to have formed abiogenically, i.e. by rapid degassing of CO_2 and concomitant precipitation of calcium carbonate. The CO_2 required for the dissolution of the carbonate host rock is either derived from the soil zone, from a deep-seated source, or a combination of both. The latter two types of travertine are often associated with hot springs in tectonically active areas (e.g., Fouke et al., 2000; Brogi, 2004).

Travertine provides valuable information about palaeohydrological and palaeoenvironmental conditions, because it may form continuously over hundreds or thousands of years thereby recording changes in water availability and climate. Mineralogy and fabrics of travertine are strongly dependent on water temperature and composition and, locally, microbial activity (Turi, 1986; Fouke et al., 2000). Regular lamination often reflects a strong annual or even diurnal control (Guo and Riding, 1994). Stable isotopic and trace element studies can provide further insights into the physical and chemical conditions of the carbonate-precipitating waters (Pazdur et al., 1988; Garnett et al., 2004a; Smith et al., 2004) if the system is well understood (cf. Chafetz and Lawrence, 1994).

In contrast to travertine, tufa is a low-temperature, low-Mg calcite deposit associated with springs, streams or waterfalls, showing a highly porous fabric due to incrustation of plant material or microbial mats (Pedley, 1990; Ford and Pedley, 1996; Pentecost, 2005). Karstification driven by soil-derived CO_2 leads to the formation of Ca-HCO_3-waters which rapidly degas at springs and/or at zones of high water turbulence along streams

(cascades, waterfalls). Carbonate precipitation is largely driven by thermodynamic supersaturation (as a result of degassing of CO_2), but plants and mosses growing at springs and in creeks provide large surfaces, thereby enhancing degassing (Arp et al., 2001). Microorganisms have a significant impact on crystal fabrics and rate of carbonate precipitation (Andrews et al., 1997; Merz-Preiß and Riding, 1999). Many tufa deposits are regularly bedded and locally also laminated (Kano et al., 2003). Some of these deposits faithfully record seasonal changes in temperature and/or rainfall variations (Matsuoka et al., 2001; Ihlenfeld et al., 2003). The potential for diagenetic alteration, however, is generally much higher in tufas than in travertine because of their generally high primary porosity and permeability.

An aspect which makes an investigation of Quaternary travertines and tufas particularly interesting is the possibility to absolutely date them using the U/Th method (Harmon et al., 1980; Sturchio et al., 1994; Eikenberg et al., 2001; Frank et al., 2000; Mallick and Frank, 2002; Garnett et al., 2004b; Wang et al., 2004). This permits palaeoenvironmental data obtained from these deposits to be tied into a chronostratigraphic frame with an upper age limit of approximately 400-500 kyr. Difficulties arise from contamination by detrital Th, low initial U concentrations and/or young sample ages (small ingrowth of radiogenic ^{230}Th). Porous tufa deposits in general are more difficult to date than compact travertine (Garnett et al., 2004b), primarily because the system remained open with respect to the radionuclides long after sedimentation.

Tufa deposits of Quaternary age are numerous in the Alps and are particularly abundant during the Holocene (Hermann, 1957; Huckriede, 1975; Jerz and Mangelsdorf, 1989; Krois et al., 1993; Pentecost, 1995; Andrews et al., 1997). Dense and well laminated travertine, however, is largely absent. This paper reports an occurrence of such a laminated travertine deposit, albeit inactive, in Eastern Tyrol which is composed of both calcite and aragonite. Using a combined field and laboratory approach involving hydro- and geochemistry we examined this carbonate deposit in an attempt to reconstruct palaeohydrological and palaeoenvironmental conditions during its formation.

2. Geologic setting

The travertine deposit is located on a steep, woody SW facing slope near Ainet (Isel Valley, Eastern Tyrol, latitude 46.86179 N, longitude 12.70262 E) at the western edge of the Schober Group between 780 and 920 m a.s.l. (Fig. 1). The area belongs to the metamorphic basement of the Austroalpine unit south of the Tauern Window. The main part consists of the Schober basement

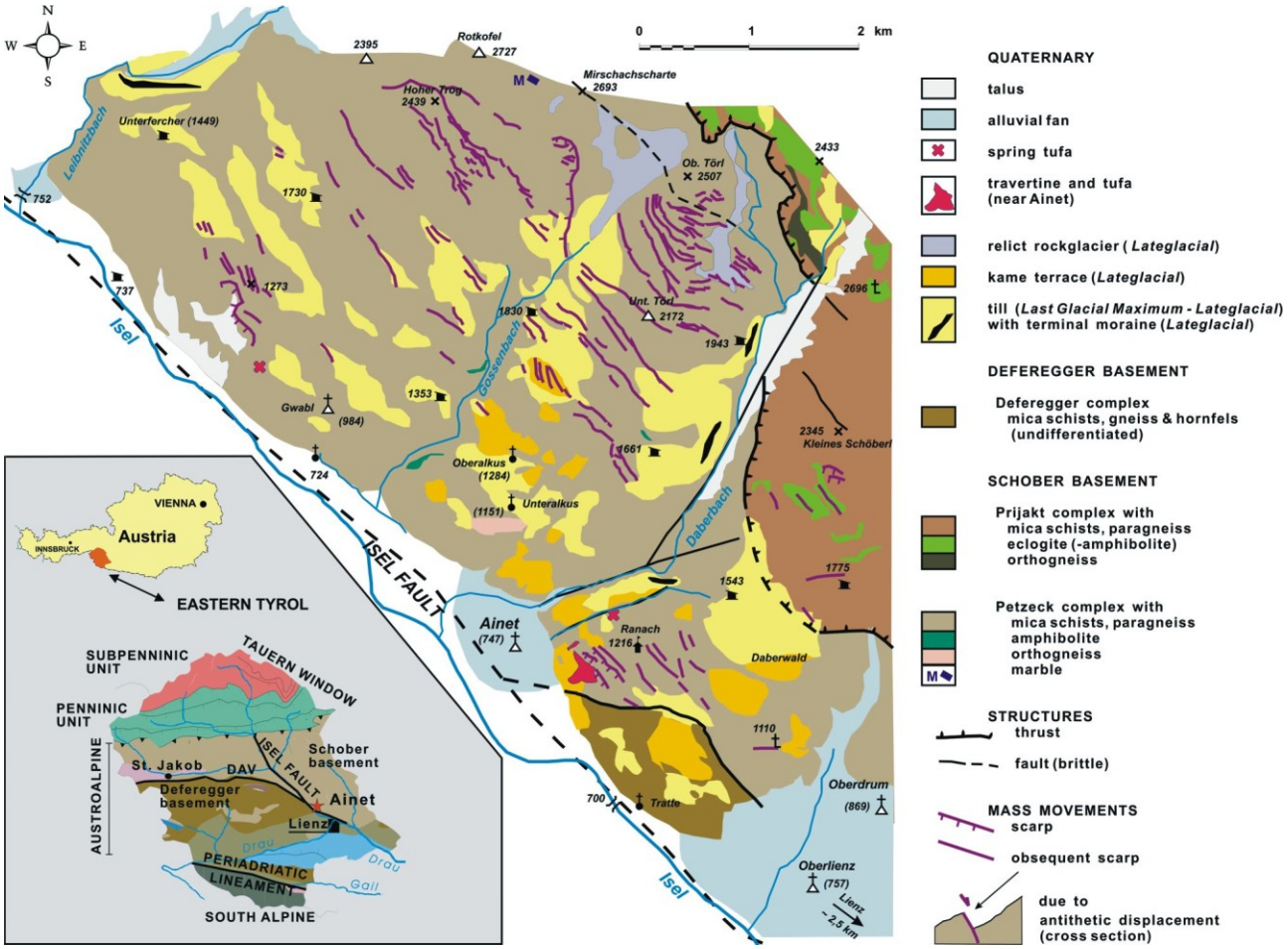

Figure 1: Geological sketch map of the southwestern part of the Schober Group showing the location of the travertine deposit near Ainet (compiled and simplified after Linner 1994, 1995b and Reitner, 2003).

which can be separated into a lower and an upper complex. A zone of imbrication showing extensive recrystallization constitutes the boundary between the two units (Troll et al., 1976). The lower Petzeck complex (Linner, 2005) — mainly present in the northern part of the Schober Group — consists of paragneis, mica schist, quartzite, orthogneiss and amphibolite, whereas the upper Prijakt complex comprises amphibolite, eclogite-amphibolite, ortho- and paragneiss (Troll et al., 1976; Linner, 1995a). The tectonic position of the Prijakt complex is supposed to be the result of N-directed overthrusting (Troll et al., 1976; Behrmann, 1990). Marble is extremely rare within the Petzeck complex and only one outcrop of a 1 m thick marble bed intercalated with metapelites was mapped on the SW flank of the Schober Group (Linner 1995a; Fig. 1). The lower part of the Schober Group between Ainet and Oberlienz consists of mica schist, gneiss and hornfels of the Deferegger Complex which belongs to the tectonic unit of the Deferegger Basement (Linner, 2005).

The NW-SE trending, dextral Isel fault running along the Isel Valley represents the morphologically dominant fault in the study area (Fig. 1). This fault is related to the Periadriatic dextral transpressive regime and, consequently, to the lateral extrusion around 17 Myr leading to the exhumation of the Tauern Window (Mancktelow et al., 2001). The Isel fault cuts the E-W trending Defereggen-Antholz-Vals (DAV) fault, which fades out W Ainet (Linner, 2005). The ductile sinistral DAV fault separating the Deferegger from the Schober basement W Isel Valley was active until around 30 Myr ago (Mancktelow et al., 2001). During the following transpressive dextral regime a reactivation of this E-W fault zone occurred resulting in polyphase brittle structures. Between Ainet and Oberlienz the Deferegger basement and the Schober basement are separated by a brittle dextral fault S Daberwald (Linner, 2005). Marbles as well as limestones are present, however, within and adjacent to the fault zone of the DAV ca. 2 km NW Ainet and on the opposite flank of the Isel Valley (Linner, 2003).

Quaternary sediments are present in the Isel Valley and along the slopes of the Schober Group (Fig. 1). These sediments are predominantly till, mostly from the Last Glacial Maximum (LGM; 19-23 kyr BP according to Mix et al., 2001), when the Isel Valley was filled by an ice stream with a surface elevation of ca. 2300 m a.s.l. (Reitner, 2003). Crudely bedded, coarse grained, poorly sorted, and unconsolidated gravel is common from 1700 m a.s.l. down to the valley floor (ca. 720 m a.s.l.), e.g. near Daberbach and Gossenbach, which are tributaries of the Isel. These sediments resemble kame terraces deposited by meltwater streams along the margin of the collapsing ice stream soon after the LGM. This was the last time when the tributary glaciers reached the lower flanks of the Isel Valley such as the glacier of the Daberbach overriding previously deposited ice-marginal sediments NW Ranach (Reitner, 2003). According to calibrated ^{14}C data from other Eastern Alpine valleys (van Husen, 2004; Reitner, 2005) the Isel Valley around Ainet was probably already ice free ca. 18 kyr BP ago. The further retreat of the local glaciers to higher cirques during the Lateglacial is documented by a series of terminal moraines (Buchenauer, 1990; Fig. 1). During this time interval the lower limit of discontinuous permafrost receeded to higher elevations, as witnessed by fossil rock glaciers (Buchenauer, 1990). In the catchment areas of the Daberbach and Gossenbach streams the lower limit of discontinuous permafrost - presently located around 2700 m a.s.l. - was situated at ca. 2100 m a.s.l. during Greenland Stadial 2 and at ca. 2200 m a.s.l during the Greenland Stadial 1 (terminology according to Björk et al., 1998).

The travertine deposit stratigraphically overlies gravel of the above described kame terraces on the lower part of the mountain slope and appears to be at the toe of a deep-seated gravitational mass movement (Reitner, 2000). The SW-facing slope above the area of Ranach (1216 m a.s.l.) is dissected by extensional graben structures and obsequent scarps giving rise to a stair-case morphology, typical of deep-seated toppling (Fig. 1). This slope failure along the SW facing flank of the Schober Group is the result of antithetic displacements along faults and joints striking parallel to the Isel fault and dipping steeply NE toward the slope (Reitner, 2000). This slope morphology suggests that the depth of rock disintegration may reach as deep as 150 m, as estimated for the slope near the Oberes Törl (Fig. 1). In analogy to other areas where this kind of mass movement was observed (Reitner et al., 1993) the toppling started as the slopes had been oversteepened by glacial erosion and had lost support during downwasting of the Isel glacier. It is important to note that the travertine deposit is disrupted by later gravitational slope movements.

3. Methods

Rock samples were obtained from both, carbonate cements within the underlying clastic ice-marginal sediments and the travertine above. Petrographical examinations included transmitted-light and epifluorescence microscopy on thin sections, as well as the determination of the mineralogical composition of the carbonate material using powder X-ray diffraction (XRD). Samples for stable C and O isotope analyses were microsampled from rock slabs at 0.1 mm increments using a semi-automated Micromill system (Merchantek) and measured using a continuous-flow isotope ratio mass spectrometer in the isotope laboratory at Leopold-Franzens-Universität Innsbruck (see Spötl and Vennemann, 2003 for analytical details). Results are reported relative to the VPDB standard. Four samples were selected for U/Th age determination, including two samples of pore-filling calcite from the underlying clastic sediments (samples Ain1 and Ain9), one calcite sample from the travertine (sample Ain6) and one travertine sample almost exclusively consisting of aragonite (Ain4). Samples were dissolved in nitric acid after adding approximately 100 mg of a mixed ^{229}Th-^{236}U spike. Th and U were separated and purified in columns containing an ion exchange resin following standard techniques (Ivanovich and Harmon, 1992). Measurements were performed using a Nu Instruments multicollector inductively coupled plasma mass spectrometer at the University of Bern, Switzerland (see Burns et al, 2003 for details). Ages and 2-sigma uncertainties were calculated using the decay constants of Cheng et al. (2000).

To clarify the modern environmental conditions in the area of the travertine deposit, field studies, including the collection of spring water samples (Fig. 2), were carried out three times during the period of investigation (July and October 2003, May 2004). Analyses of the water samples included field measurements of electric conductivity, carbonate alkalinity and pH. Concentrations of cations (Na, K, Ca, Mg, Sr) and anions (F, Cl, NO_3, SO_4), as well as the concentrations of dissolved SiO_2 were measured in the laboratory using standard techniques (cations: University of Innsbruck; anions: Keele University/UK; dissolved SiO_2: Natural History Museum Vienna). Thermodynamic calculations were performed using PHREEQC. In addition, the C isotopic composition of dissolved inorganic carbon ($\delta^{13}C_{DIC}$) was determined using a gas evolution method based on continuous-ousflow technology and reported relative to VPDB (see Spötl, 2005 for analytical details). The O isotopic composition of the water samples was determined using the CO_2 equilibration method and results are reported relative to the VSMOW standard. Precision (1 sigma) is better than 0.1 ‰.

4. Results

4.1. Field studies

Field investigations show that the ice-marginal sediments of the kame terrace underlying and adjacent to the travertine deposit are strongly cemented (Fig. 3A). In addition, massively cemented patches of coarse grained clastic sediments (ice-marginal sediments probably intermixed with talus) are present higher up on the slope. Within the glacial sediments isopachous calcite rinds in porous gravel as well as flowstone-like layers of calcite are present in fractures (Fig. 3A). These calcite layers reach a thickness of up to 40 cm (typically a few centimetres) and caused localized consolidation of the otherwise unconsolidated ice-marginal sediments.

The travertine sharply overlies the consolidated gravels (Fig. 3B) and consists of a lower interval (ca. 2.5 m) of compact and regularly laminated carbonate, lacking siliciclastic inclusions. The travertine grades upward into progressively more porous and less distinctly laminated travertine. The uppermost 10 to 20 cm are highly porous tufa containing imprints of leaves and casts of grasses and needles. Although the travertine deposit has been fractured and partially disintegrated due to slope processes subsequent to its formation, there is clear field evidence of synsedimentary bending of the strata on metre-scale at the edge of the small terrace formed by slope movements (Fig. 3C). These primary sedimentary features resemble barrages commonly observed in modern tufa and travertine occurrences (e.g. Andrews et al., 2000).

The travertine body is clearly inactive today and covered by brown soil and vegetation (forest) and partially disintegrated into individual blocks (Fig. 3D). Hydrological activity in the vicinity of the travertine body is limited to streams which, although mildly supersaturated with respect to calcite (see Hydrochemistry, below), lack visible carbonate precipitation. Small, isolated occurrences of inactive spring tufa (Fig. 1) are also present in other places along the slope of the Schober Group (Reitner, 2003).

4.2 Mineralogy and Fabrics

The bulk of the travertine deposit consists of regularly laminated, dense carbonate material. White radiaxial, fibrous aragonite layers (confirmed by XRD analyses) alternate with typically thinner, light brown, fibrous calcite layers resulting in a macroscopically visible millimetre-scale rhythmite (Figs. 4A, B). Additionally, micrometre-thin micrite layers, which often pass laterally into the fibrous calcite layers, are present. Lamina thickness varies between 0.1 and 2 mm for both aragonite and calcite laminae, although aragonite laminae are typically thicker. Within the aragonite layers hemispherical aggregates are a common feature (Figs. 4B, C). These aggregates show a distinct, micrometre-scale lamination. Observations using epifluorescence suggests that this fine lamination is caused by a regular alternation of brightly fluorescent and dull fluorescent laminae (Fig. 4D). Up to 150 individual laminae are present within a ca.

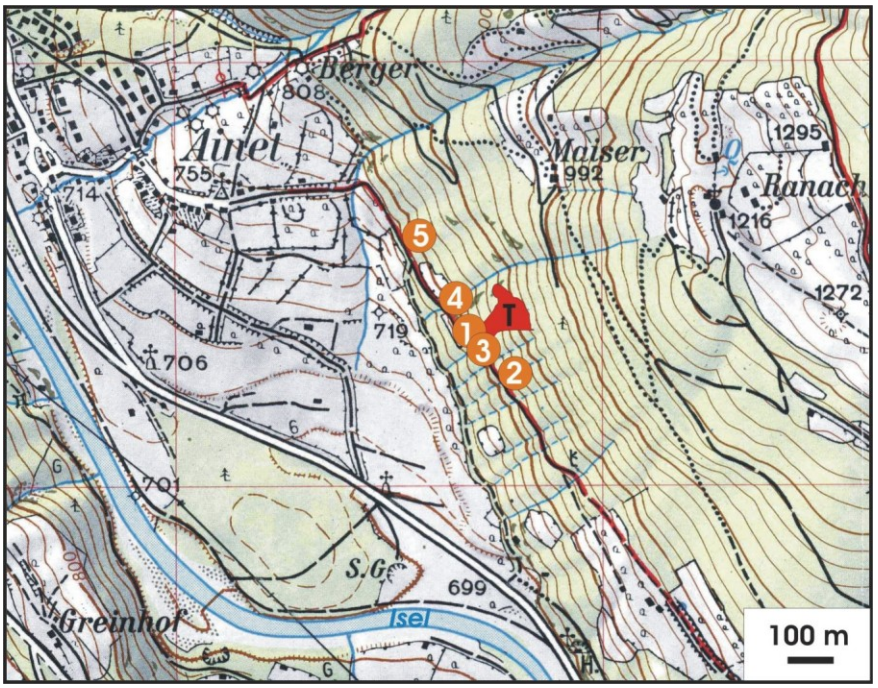

Figure 2: Geographic map of the area near Ainet showing location of water sampling sites in relation to the travertine occurrence (T). Reproduced with permission of the BEV - Bundesamt für Eich- und Vermessungswesen, Vienna, EB 2005/01576.

1 mm thin layer. This fine lamination can also be observed in the fibrous calcite layers, albeit less distinct. Aragonite layers locally show evidence of partial dissolution (Figs. 4B and C). Shrub-like aggregates of a second generation of aragonite crystals are present in voids. Locally, fractures (both subhorizontal and obliquely oriented) within the calcite-aragonite succession are filled by isopachous, brown and dense calcite rinds showing bipolar growth textures and lamination. These fracture fills are identical to the isopachous calcite cement in the clastic sediments forming flowstone-like deposits locally up to 40 cm in thickness.

Within the uppermost part (i.e. some tens of centimetres beneath the surface) the travertine changes from dense, well laminated into porous and less distinctly laminated (Fig. 4E). Thick, porous, mixed aragonite-calcite layers alternate with thinner, dense calcite layers. The abundance of siliciclastic material, plant casts and imprints increases up section within this interval, which then passes gradually into highly porous tufa (Fig. 4F). This topmost unit contains abundant sand- and silt-size detritus as well as encrusted plant material, and is composed of calcite only.

4.3 Carbonate stable isotope analysis

Stable C and O isotope analyses of aragonite range from +1 to +2 ‰ and -10.4 to -9.6 ‰, respectively, while those of calcite vary only between -1.8 to 0 ‰ and -11.2 to -10.5 ‰, respectively. C and O isotope values show strong covariance with a slope $\Delta\delta^{13}C/\Delta\delta^{18}O$ of 2.4 (Fig. 5). High-resolution isotope traverses across regularly laminated travertine show a near-rectangular pattern of low calcite values and high aragonite values (Fig. 6). Due to the slightly irregular boundaries between individual calcite-aragonite laminae micromilling resulted in variable admixing of calcite near aragonite boundaries giving rise to more gradual isotope shifts. Isotopic measurements of porous, calcitic tufa yielded values of -3 to -2 ‰ for $\delta^{13}C$ and -12 to -11 ‰ for $\delta^{18}O$

Figure 3: Features of the travertine in the field. (A) Isopachous calcite cemented ice-marginal sediments, (B) Bedded travertine conformably overlying cemented clastic sediments. Arrow indicates boundary between the two units. (C) Inclined beds at the former edge of the travertine terrace. The strata were later disrupted by gravitational slope processes. Hammer for scale. (D) Overview of the major outcrop of the laminated travertine body. Note the stratified nature of the deposit. Rucksack for scale.

(Fig. 5), which are clearly lower than those of the laminated (calcite) samples.

4.4. Hydrochemistry

Waters from five streams in the vicinity of the travertine deposit (Fig. 2) show elevated values of electrical conductivity (400-530 µS/cm) and carbonate alkalinity (9-13 °dH; Table 1). Cation analyses yielded elevated Mg and Sr concentrations (22-35 mg/l and 0.3-0.5 mg/l, respectively), as well as relatively high K/Na and Mg/Ca ratios (both 0.6 to 0.8). Anions show elevated SO_4 and

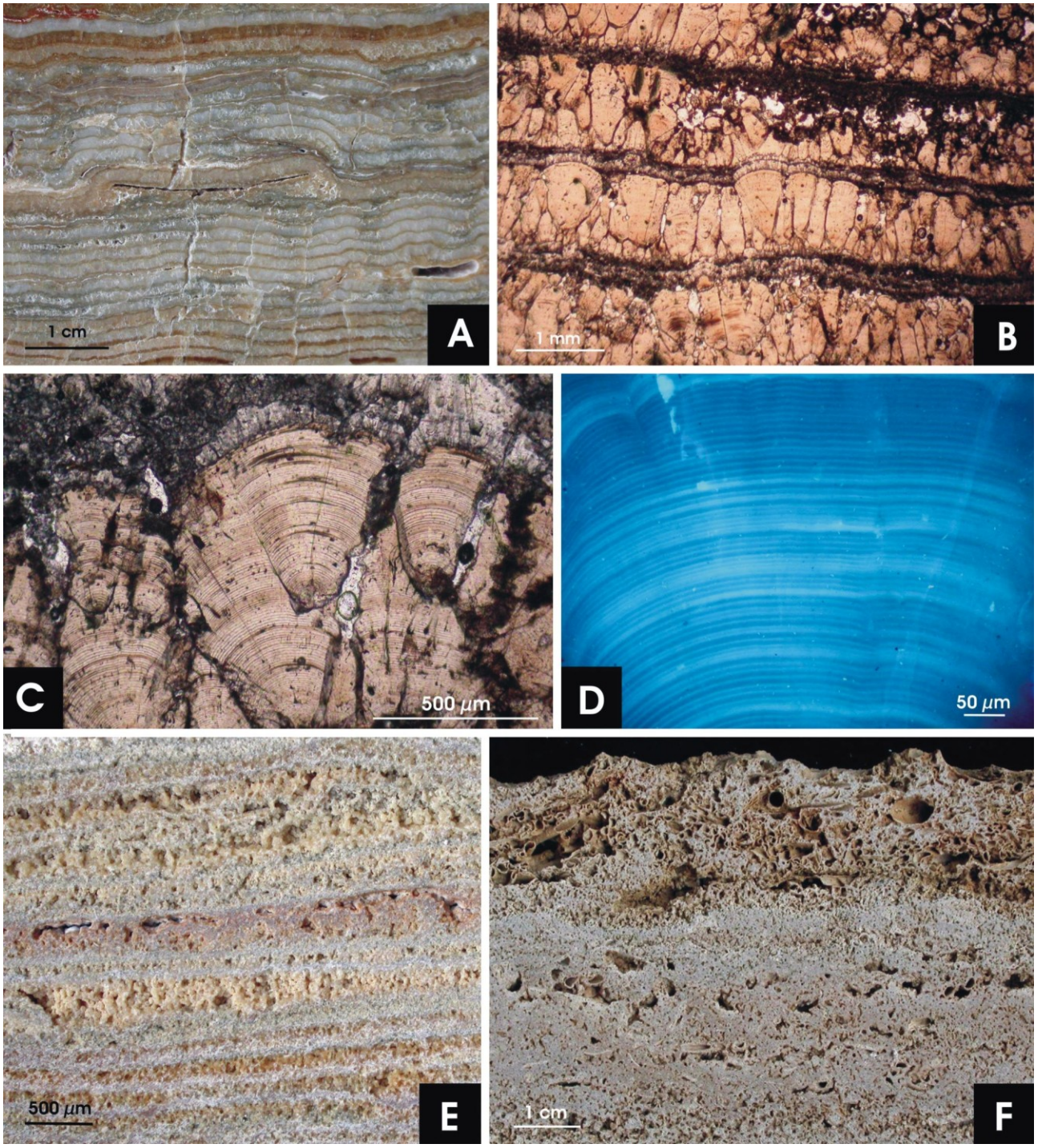

Figure 4: Macroscopic and microscopic features of the travertine. (A) Polished section of an aragonite (white)-calcite (light brown) rhythmite. Note laminae draping over a former leaf (cast in centre of image). (B) Thin section of aragonite-calcite couplets. Note hemispheric growth form of aragonite and evidence of dissolution near the upper right-hand corner. Transmitted-light photomicrograph, parallel nicols. (C) Aragonite hemispheres showing fine-scale, concentric lamination of presumably diurnal origin. Note corrosion features between adjacent aragonite aggregates. Transmitted-light photomicrograph, parallel nicols. (D) Close-up of an individual aragonite hemisphere composed of numerous growth laminae under blue-light epifluorescence. The bright fluorescing laminae correspond to light brown laminae as seen in normal transmitted light. (E) Transition between bedded, dense travertine to calcite tufa composed of porous aragonite and less porous calcite layers. (F) Calcite tufa from the top of the travertine body.

F contents (50-63 mg/l and 0.2-0.4 mg/l, respectively). Values of dissolved silica range from 7.4-10.4 mg/l. All water samples except one are clearly supersaturated with respect to calcite (saturation index (SI) up to 0.96) and aragonite (SI up to 0.81) with higher SI values during summer (Table 1). Values of -log pCO_2 calculated from the chemical analyses range from 3.4 to 2.6, i.e. slightly higher than the atmospheric value (Table 1). $\delta^{13}C_{DIC}$ values range from -8 to -6 ‰. Oxygen isotope values show little variation (-12.1 to -11.5 ‰, mean -12.0 ‰), suggesting a high mean altitude of the water infiltration.

4.5. Age determination

Four carbonate samples dated using the U/Th method yielded Lateglacial ages (Table 2). A calcite sample from the top of the laminated succession (Ain6) and a predominantly aragonite sample from the central part (Ain4, containing minor amounts of calcite) show ages of 13.44 ± 0.16 kyr BP and 13.49 ± 0.17 kyr BP, respectively. Two samples of calcite cement (Ain1 and Ain9) from the underlying ice-marginal sediments show slightly older ages (13.69 ± 0.13 kyr BP and 13.96 ± 0.11 kyr BP). All samples exhibit very high U concentrations of approximately 200 ppm regardless of the mineralogical composition and the ^{232}Th correction is therefore negligible.

5. Discussion

5.1 Setting of the travertine

The travertine deposit located on a SW facing slope E Ainet is an isolated occurrence which was first discovered during routine geological mapping (Reitner, 2003). So far, it is the only such body in this area and we are unaware of comparable deposits in other regions of the Eastern Alps. The deposit is petrologically distinct from spring tufas and in fact gradually evolves into tufa up section. This suggests that the mode of formation of this travertine may not be directly comparable to (modern) tufa deposition. Although the majority of the deposit is hidden beneath forest soil, gravitational mass wasting and slope erosion provide local access to the internal structure of the travertine. These observations suggest that the waters first percolated through coarse-grained clastic sediments thereby precipitating isopachous calcite rinds. Subsequent carbonate precipitation occurred subaerially (and continued locally in the subsurface), giving rise to a travertine terrace forming on top of cemented clastic sediments. There is evidence of cascade- or barrage-like structures near the edge of the terrace (cf. Fouke et al., 2000), but the distal part of the deposit (further down the slope) is not preserved. Biological structures (e.g., casts of leafs) are not abundant within the main body of the travertine, unlike modern (and Holocene) tufa deposits which engulf trees and calcify mosses and grasses. The abundance of casts of grasses and imprint of needles in the top tufa layer, however, suggests an increase in local vegetation toward the end of travertine accretion.

No modern tufa or travertine formation occurs today, although streams in the vicinity of the deposit are mostly supersaturated with respect to calcite and even aragonite (Table 1). Small patches of tufa are present in the area (Fig. 1) and may have formed during the Early Holocene, but dating control is lacking. In summary, field evidence documents that the groundwater discharge that lead to the formation of bedded travertine near Ainet was a comparably short-lived event after deglaciation of the Isel Valley.

5.2 Internal structure of the travertine

The most conspicuous aspect of the deposit are the calcite-aragonite couplets which constitute the main part of the succession (Figs. 4A, B). Both, the white aragonite and the light brown, fibrous calcite are of primary origin and we rarely found thin-section evidence of minor replacement of aragonite by calcite. The regular interlayering of these two polymorphs also

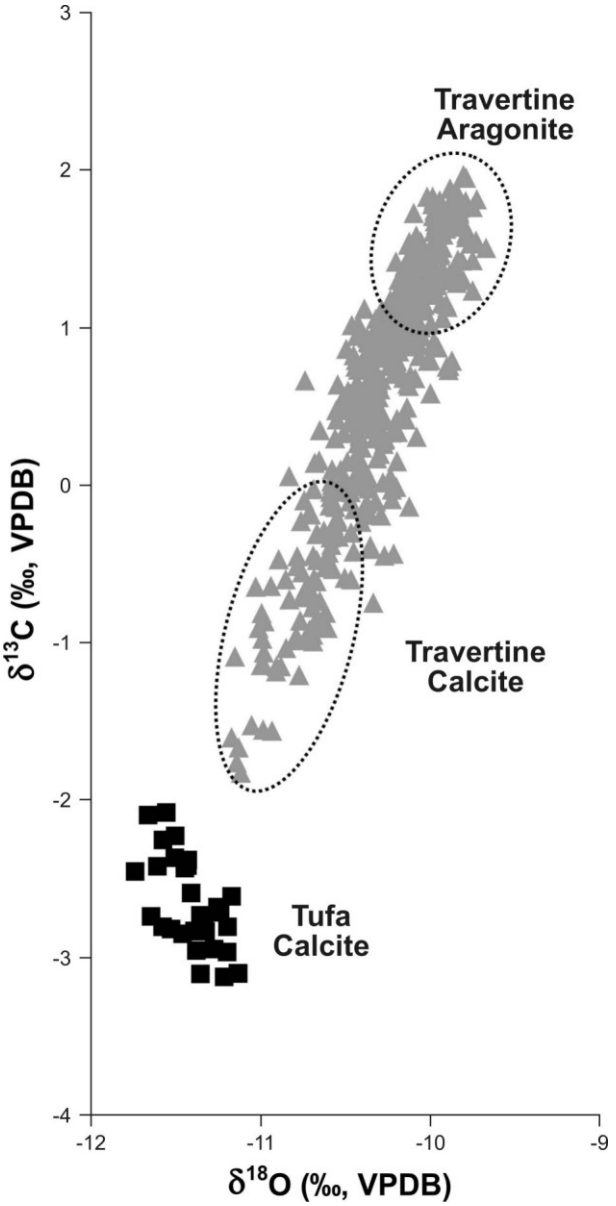

Figure 5: Stable isotopic analyses of travertine and tufa samples from Ainet. The two circles define the compositions of aragonite and calcite endmembers. For details see text.

argues in favour of a primary sedimentary origin, similar to calcite-aragonite preserved in speleothems (Railsback et al., 1994). While abundant in the rhythmite succession, aragonite is not present within the clastic sediments beneath and adjacent to the travertine body, which are cemented by vadose isopachous calcite rinds only. The groundwater seeping through the clastic sediments apparently never reached the supersaturation required for aragonite to precipitate.

Sample	Site	Temp.	Cond.	Carb. Alk.	pH	Cations (mg/l)					Anions (mg/l)							SI_{Cc}	SI_{Arag}	-log pCO2	$\delta^{13}C_{DIC}$	$\delta^{18}O_{Water}$
		(°C)	(µS/cm)	(°dH)		Na	K	Ca	Mg	Sr	F	Cl	NO_3	SO_4	HCO_3	SiO_2					(‰, VPDB)	(‰, VSMOW)
01.07.2003																						
WAin1	1	9,2	470	11,8	8,41	7,3	4,9	47,3	34,1	0,43	0,23	1,01	0,44	59,3	257,1	8,1	0,76	0,60	3,12		-6,76	-11,97
WAin2	2	17,0	530	13,2	8,10	7,9	5,9	60,7	34,3	0,47	0,24	0,69	0,13	62,9	287,7	10,4	0,72	0,57	2,72		-10,56	-11,50
WAin3	3	9,7	480	11,6	8,46	7,1	5,0	47,7	34,9	0,43	0,31	0,82	0,40	58,8	252,8	8,2	0,81	0,66	3,17		-6,56	-12,12
WAin4	4	11,0	493	11,8	8,44	6,5	4,5	52,8	34,4	0,42	0,44	1,02	0,30	57,8	257,1	8,1	0,86	0,71	3,14		-7,42	-12,02
WAin6	5	12,2	404	9,2	8,48	4,2	4,1	49,9	21,6	0,30	0,15	0,79	0,49	53,0	200,5	7,8	0,81	0,66	3,28		-7,80	-12,08
29.10.2003																						
WAin8	1	7,8	488	11,5	8,23	6,2	4,3	47,3	34,1	0,43	0,23	0,76	0,62	61,9	250,6	7,8	0,55	0,40	2,95		-6,70	-11,98
WAin9	2	5,9	472	10,7	7,85	5,9	4,3	50,0	30,0	0,38	0,26	0,93	0,11	62,9	233,2	7,5	0,14	-0,02	2,62		-7,19	-11,98
WAin10	3	7,7	483	11,4	8,29	6,5	4,4	46,9	33,9	0,42	0,22	0,69	0,44	60,2	248,4	8,0	0,60	0,45	3,02		-6,65	-12,10
WAin11	4	7,4	490	11,6	8,37	6,9	4,9	51,1	33,1	0,41	0,23	0,70	0,00	59,9	252,8	7,9	0,72	0,56	3,09		-6,50	-12,09
WAin13	5	6,7	403	9,2	8,31	4,6	4,5	50,3	21,9	0,30	0,28	0,73	0,00	48,5	200,5	7,4	0,57	0,41	3,13		-7,27	-12,10
04.05.2004																						
WAin15	1	7,5	490	11,8	8,50	6,5	4,4	47,8	35,5	0,40	0,21	0,67	0,49	58,9	257,1	8,0	0,82	0,67	3,22		-6,27	-12,01
WAin16	2	8,2	491	12,0	8,10	6,1	4,5	54,6	32,2	0,38	0,23	0,45	0,03	57,2	261,5	8,4	0,51	0,35	2,81		-8,15	-11,58
WAin17	3	7,7	486	11,6	8,51	6,8	4,4	45,6	34,2	0,39	0,24	0,69	0,49	58,0	252,8	7,9	0,81	0,66	3,23		-6,26	-11,98
WAin18	4	8,0	489	12,0	8,60	6,1	4,2	51,1	33,5	0,38	0,24	0,55	0,37	57,2	261,5	8,1	0,96	0,81	3,31		-6,26	-11,95
WAin19	5	8,0	400	9,4	8,58	4,5	3,9	49,8	21,5	0,27	0,10	0,77	0,12	47,5	204,8	7,4	0,85	0,70	3,39		-6,63	-11,90

TABLE 1: Hydrochemical data of small streams in the vicinity of the inactive travertine deposit. See Figure 2 for locating of sites.

The highly regular alternation of the two $CaCO_3$ polymorphs on a scale of a few millimetres suggests a strong, high-frequency forcing, most likely of seasonal origin. Annual banding has commonly been reported from tufa and travertine deposits alike and is mostly attributed to seasonal variations in temperature and/or rainfall (Renaut and Jones, 1997; Kano et al., 2003; Ihlenfeld et al., 2003). The growth rates observed in Ainet are comparable to those from tufa occurrences (e.g., 4 mm/yr in SW Japan; Kano et al., 2003), and rather similar to the travertine deposit at Rapolano Terme, Italy (ca. 0.5 mm/yr – Guo and Riding, 1992). On the other hand, hot-spring travertine may show much faster growth rates. Chafetz and Guidry (2003) reported growth rates of more than 10 mm/yr from Mammoth Hot Springs, Yellowstone National Park, and Fouke et al. (2000) showed evidence of even higher rates from another section in the same region (several cm/yr).

As aragonite is favoured over calcite at higher temperatures (and higher Mg/Ca ratios in the water – Morse and Mackenzie, 1990) we attribute thick aragonite laminae to warm-season precipitation. Conversely, the typically much thinner low-Mg calcite laminae probably formed during the cold season, when the degree of supersaturation was lower, suppressing aragonite precipitation (e.g. Chafetz et al., 1991; Guo and Riding, 1992). Several studies conducted on travertines also suggest a possible biotic control on aragonite formation (e.g. Guo and Riding, 1992; Chafetz and Guidry, 2003). Photosynthetically active bacteria influence the degree of supersaturation by changing the CO_2 content of the water (Buczynski and Chafetz, 1991). However, both models are consistent with aragonite precipitation during the warm season and the lack of aragonite in the cemented clastic sediments beneath and lateral to the travertine body (lower temperatures in the vadose zone than at the surface).

An even finer-scale lamination is preserved in aragonite and many calcite layers (Figs. 4C, D). This lamination is not commonly seen in travertine and tufa deposits elsewhere. Given that the individual aragonite and calcite laminae are probably of seasonal origin, we regard the micrometre-scale lamination as most likely of diurnal origin. This interpretation is consistent with lamina counts (see above) and the presence of very thin fluorescent sublaminae (Fig. 4D). Folk et al. (1985) and Guo and Riding (1992) reported laminae from Italian travertine and attribute their origin to changes in the activity of photosynthetic bacteria due to diurnal variations in the intensity of sunlight and probably temperature (they did not report fluorescence properties, though).

The presence of rather regular lamination on millimetre and micrometre scales permits some first-order estimates of the duration of travertine formation. The average thickness of aragonite-calcite couplets is 1.5 mm, which suggests that the ca. 2.5 m thick bedded travertine terrace formed within less than ca. 1700 yr.

5.3 Stable isotopes as palaeoenvironmental proxies

The stable isotope values of C and O help to elucidate the processes involved in aragonite and calcite precipitation. The delicate interlayering of aragonite and calcite on millimetre scale demanded a spatially resolved sampling strategy. Despite applying high-resolution micromilling the measurements require careful evaluation prior to interpretation. The high-resolution isotope traverses show a steep rise in both isotope parameters at the bottom of each aragonite lamina followed by a short plateau-like feature and a steep drop near the boundary to the next calcite lamina (Fig. 6). Close inspection reveals, however, that this isotope pattern results from inevitable mechanical mixing due to the finite width of the milling trench. The more irregular the boundaries of the aragonite-calcite couplets (in three dimensions) the more gradual the apparent isotope shifts. We therefore regard only isotope values from the centre of each lamina as reliable and regard data from those few laminae that do not run strictly perpendicular to the direction of the sampling trench as mixtures. Within the central portions of the aragonite laminae there is little (<0.5 ‰) systematic change in $\delta^{18}O$ (Fig. 6). This intra-lamina isotope variability is smaller than the inter-lamina variability.

When plotted on a standard scatter diagram the stable isotope data define a band showing a high degree of linear correlation (Fig. 5). This essentially reflects the covariance seen in the stable isotope traverses and therefore represents a binary (artificial) mixing line only.

At equilibrium conditions (25°C) aragonite is expected to be enriched in ^{18}O relative to coexisting low-Mg calcite by 0.6 ‰ (Tarutani et al., 1969). Frisia et al. (2002) reported a mean value of 1 ‰ (range 0.7 to 1.4 ‰) for aragonite-calcite speleothem samples from southern France. Pure aragonite layers from Ainet are on average ca. 0.8 ‰ higher in ^{18}O compared to calcite layers, suggesting that both polymorphs formed from spring water of similar O isotopic composition.

This interpretation can be tested by comparing the stable C isotopic compositions of aragonite and calcite. According to equilibrium considerations aragonite is enriched in ^{13}C relative to co-precipitating calcite at 25°C by 1.7 (±0.4) ‰ (Romanek et al., 1992). Speleothem samples studied by Frisia et al. (2002) showed a slightly higher ^{13}C enrichment (2 to 3.4 ‰), attributed to additional kinetic fractionation during aragonite precipitation. Figure 5 shows that $\delta^{13}C$ values of aragonite from Ainet are on average ca. 2 to 2.5 ‰ higher than those of the calcite laminae, supporting our previous interpretation that no significant change in the isotopic composition of the water occurred during the seasonal shift from aragonite to calcite precipitation. Taking together, these data also argue against significant kinetic fractionation during carbonate precipitation. This is an important conclusion, as it rules out evaporation as a major driving force of aragonite precipitation. In addition, some quantitative constraints can be placed on the conditions of carbonate formation at Ainet. If we assume that the palaeowaters had a $\delta^{18}O$ value similar to today's streams in the area (-12 ‰) the calculated equilibrium water temperature was <10°C for both aragonite and calcite. These values are sufficiently close to the mean annual air temperature (ca. 7°C) and to the measured water temperatures of streams in this area (see Table 1) to render a hydrothermal origin of the travertine-forming water unlikely.

A simple sensitivity test corroborates the robustness of these findings. Calculations of the $\delta^{18}O$ value of water in isotopic equilibrium with the observed aragonite isotope values at elevated temperatures (assuming 25-30°C) yield -6.7 to -5.6 ‰

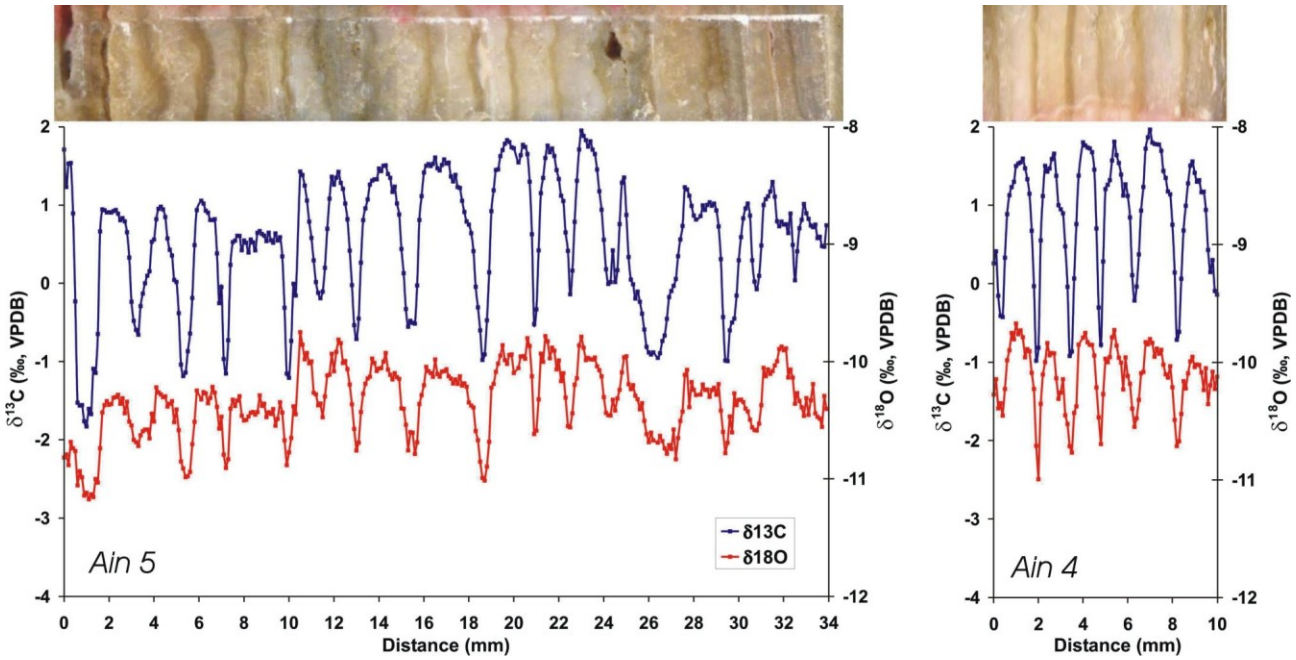

Figure 6: Continuous, high-resolution stable isotope traverses across two laminated aragonite-calcite travertine samples. Aragonite laminae are milky white, thinner calcite laminae are brownish. Note correspondence between the shape of the isotope profile and the geometry of the laminae.

(Zhou and Zheng, 2003). These values are much higher than today's spring water composition and are very difficult to explain in this inneralpine setting. Conversely, the O isotope composition of calcite constrains the water $\delta^{18}O$ value to -8.5 to -7.5 ‰, again rather unrealistically high values for this region (see also Zötl and Goldbrunner, 1993 for an up-to-date summary of O isotope data on a variety of springs in the Alpine region).

The O isotopic composition of the tufa capping the travertine deposit is lower than that of the calcite in the rhythmite succession by up to 1 ‰ and shows no covariance with $\delta^{13}C$ (Fig. 5). Using the tufa $\delta^{18}O$ values and the mean $\delta^{18}O$ value of modern streams in the area (-12 ‰) equilibrium palaeowater temperatures of ca 10-13°C can be obtained (using Kim and O'Neil's 1997 relationship). Although these values are higher than today's mean annual air temperature (ca. 7°C), they are consistent with tufa formation that occurred preferentially during the warm season, when both air temperatures and photosynthetic activity were high.

The C isotopic compositions of both the rhythmically bedded travertine and its tufa cap show elevated $\delta^{13}C$ values (Fig. 5), significantly higher than those reported from most modern tufas in climatically comparable regions (see review in Andrews and Brasier, 2005), but consistent with a compilation of data from travertine deposits (Turi, 1986). These values indicate that DIC of the palaeowater was largely rock-buffered (there is only a small (<1 ‰) fractionation between DIC and calcite – Romanek et al., 1992). In contrast, $\delta^{13}C_{DIC}$ values of streams in the area are significantly lower (-8 to -6 ‰) reflecting a higher proportion of soil-derived DIC in the present-day groundwater. In other words, the C isotope data suggest a change in groundwater composition between the time of travertine deposition and today.

What controlled the regular switching between aragonite and calcite precipitation? We argued above that these couplets are most likely of annual origin, an assumption that is largely consistent with the duration of travertine deposition as suggested by the U/Th data. The switch from metastable aragonite to low-Mg calcite precipitation is probably related to seasonal changes in air temperature, but the precise mechanism remains unclear. Solar heating of the water (SW exposed location) may have facilitated aragonite precipitation during summer (Morse and Mackenzie, 1990), whilst cold temperatures and partially freezing conditions during the months of November through April resulted in thin laminae of calcite. The stable isotope data, however, rule out significant evaporative concentration of the solution as a means to promote aragonite over calcite precipitation. Seasonally changing pCO_2 of the discharging groundwater could also influence the saturation state of groundwater as enhanced biological activity in the soil zone during summer gives rise to more CO_2 being dissolved in the groundwater (cf. Kano et al., 2003). Stable C isotope data, however, suggest that the proportion of the latter was low (see above), i.e. the C system was largely rock-buffered and insensitive to seasonally variable input of soil-CO_2. Bacteria may also influence crystal nucleation in travertine deposits, both actively and passively (Merz-Preiß and Riding, 1999; Fouke et al., 2000; Chafetz and Guidry, 2003; Kano et al., 2003) and it is conceivable that cyanobacterial activity during the warm season enhanced abiogenic degassing of CO_2, thereby favouring aragonite over calcite precipitation. Guo and Riding (1992) reported regularly alternating aragonite-calcite lamination from Italian travertines and suggest a biotic control on aragonite formation, whilst calcite is apparently of abiotic origin.

5.4. Origin of palaeofluid flow

The stable O isotope data of the travertine suggest that the palaeowaters were isotopically similar to present-day springs and streams on the flank of the Schober Group, i.e. they were recharged as meteoric precipitation higher up on the mountains. Hydrochemical data show that today's streams contain an appreciable amount of total dissolved solids, expressed as electric conductivity values up to 530 µS/cm (Table 1), even exceeding values typical of aquifers in limestones of the Alps (e.g., Zötl and Goldbrunner, 1993). These high values in conjunction with high concentrations of dissolved silica and elevated concentrations of F and sulfate (Table 1) are fingerprints of rather extensive water-rock interactions in the aquifer of these metamorphic rocks even today. The very high U content of the travertine (both in aragonite and calcite – Table 2) as well as the high $\delta^{13}C$ values underscore this conclusion. Geologic mapping revealed only a single small outcrop of a marble lense on the flank of the Schober Group (Linner, 1995a; Fig. 1). Present-day water compositions of the streams are also more consistent with extended leaching of carbonate-poor metamorphic rocks: the molar Ca(+Mg)/HCO_3 ratio is 0.61-0.66, inconsistent with simple stoichiometric dissolution of carbonate rocks. Elevated sulfate concentrations hint toward sulfide oxidation as a powerful process speeding up mineral dissolution.

The most likely mechanism giving rise to such evolved water compositions in metamorphic rocks are water-rock interactions in a heavily fractured aquifer, providing large, fresh surfaces. An example of carbonate precipitation associated with metamorphic rocks are Lateglacial and Holocene calcitic and aragonitic

Sample	Description	U (ppm)	$^{234}U/^{238}U$ initial (activity)	$^{234}U/^{238}U$ (activity)	$^{230}Th/^{232}Th$ (activity)	$^{230}Th/^{234}U$ (activity)	Age (uncorr.) (years)	Age (corr.) (years)
Ain 1	Calcite cement	208.9 ± 1.0	0,9771 ± 0.0012	0,9780 ± 0.0012	1484 ± 15	0,1178 ± 0.0010	13700 ± 130	13690 ± 130
Ain 9	Calcite cement	193.9 ± 0.8	0,9794 ± 0.0012	0,9802 ± 0.0012	2119 ± 21	0,1200 ± 0.0009	13960 ± 110	13960 ± 110
Ain 6	Travertine calcite	227.6 ± 1.0	0,9786 ± 0.0015	0,9794 ± 0.0015	70426 ± 1543	0,1158 ± 0.0013	13440 ± 160	13440 ± 160
Ain 4	Trav. aragonite	190.3 ± 0.9	0,9887 ± 0.0011	0,9891 ± 0.0011	1200 ± 21	0,1162 ± 0.0014	13490 ± 170	13490 ± 170

Table 2: U/Th data

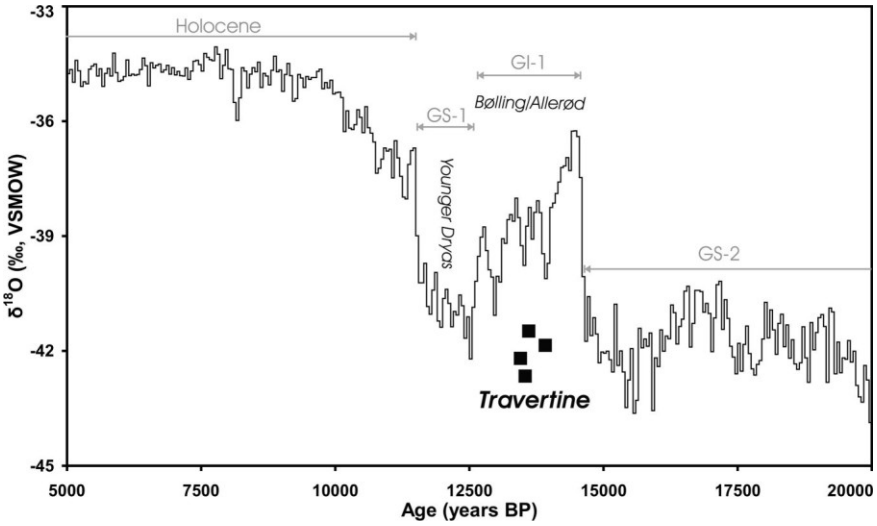

Figure 7: U/Th ages of the travertine compared to the climate evolution during the last glacial-interglacial transition as depicted by oxygen isotope data from Greenland ice core samples (North Greenland Ice Core Project Members, 2004; note that the travertine data (ages) are not referenced to the ice-core oxygen isotope scale). The errors of the U/Th analyses are within the size of the symbols (black squares). Stratigraphic terminology according to Björk et al. (1998): GS-2 = Greenland Stadial 2, GI-1 = Greenland Interstadial 1, GS-1 = Greenland Stadial 1.

flowstones in extensional joints of the heavily deformed Vinschgau schists, Southern Tyrol (Spötl et al., 2002). These speleothems are likewise very high in U and appear to be related to tufa mounds on the surface. In the case of Ainet there are two possible candidates of fractures, tectonic fractures, and fractures associated with deep-seated gravitational mass movements on the steep SW-facing flank of the Schober Group. Fractures of tectonic origin are undoubtedly present in the area (see Geologic setting) and may have facilitated fluid flow in the subsurface. The study area is situated southeast of the termination of one of the major faults in southern Austria, the DAV fault. Recent drilling for thermal waters in St. Jakob (Defreggen Valley), located 29 km WNW Ainet, encountered water of 29.5°C in strongly deformed metamorphic rocks of the DAV fault at a depth of 98 m (H. Mostler, pers. comm. 2005). Although the amount of water produced by this well was small, it proved that advective heat transport occurs along this fault zone. The chemical composition of this water, particular from a sample taken at a depth of 1.5 km, is very different from those near Ainet (electric conductivity 10.8 mS/cm, F-rich Na-Cl water type). No evidence of travertine deposition possibly associated with the DAV fault has been reported so far. The faults present in the immediate vicinity of Ainet are related to the Isel fault (Linner, 2005), but there is no clear relationship between these faults and the location of the travertine deposit.

In contrast, field studies have shown that the mountain slope above the travertine is dissected by extensional graben structures and NW-SE trending obsequent scarps (i.e., parallel to the Isel Valley; Fig. 1) leading to a stair-case like slope morphology. These features are the result of toppling due to antithetic displacement of faults and joints orientated parallel to the Isel fault and dipping toward the slope. The location of the travertine body on one of these small stair-case terraces implies a connection between its formation and the presence of fractures resulting from slope movement, as suggested by Linner (2005) on the base of mapping. These fractures may have provided new pathways for groundwater to discharge near the foot of the mountain. U/Th data tightly constrain the formation of these carbonates to the Greenland Interstadial 1 (Allerod; Fig. 7), i.e. only a few thousand years subsequent to the completing of the downwasting of the ice masses that filled the Alpine valleys during the Last Glacial Maximum (van Husen, 2004). Both, the timing of the onset of travertine deposition and its short life span as indicated by the small size of the deposit and lamina counts are consistent with a model of slope movement initiated by the melting of the valley glacier and concomitant opening of new fluid pathways allowing groundwater to emerge and precipitate carbonate locally.

6. Acknowledgements

The study was partially supported by grant Y122-GEO from the Austrian Science Fund. We would like to acknowledge M. Wimmer for laboratory assistance, R. Pavuza for silica analyses, M. Linner for sharing unpublished mapping data and H. Mostler for discussion about the drill site in St. Jakob. The authors also wish to thank M. Wagreich and A.-Voica Bojar for review and improvement of the script.

References

Andrews, J.E., Riding, R. and Dennis, P.F., 1997. The stable isotope record of environmental and climatic signals in modern terrestrial microbial carbonates from Europe. Palaeogeography, Palaeoclimatology, Palaeoecology, 129, 171-189.

Andrews, J.E., Pedley, H.M. and Dennis, P.F., 2000. Palaeoenvironmental records in Holocene Spanish tufas: a stable isotope approach in search of reliable climatic archives. Sedimentology, 47, 961-978.

Andrews, J.E. and Brasier, A.T., 2005. Seasonal records of climatic change in annually laminated tufas: short review and future prospects. Journal of Quaternary Science, 20, 411-421.

Arp, G., Wedemeyer, N. and Reitner, J., 2001. Fluvial tufa formation in a hard-water creek (Deinschwanger Bach, Franconian Alb, Germany). Facies, 44, 1-22.

Behrmann, J., 1990. Zur Kinematik der Kontinentkollision in den Ostalpen. Geotektonische Forschungen, 76, 1-180.

Björk, S., Walker, M.J.C., Cwynar, L.C., Johnsen, S., Knudsen, K-L., Lowe, J.J., Wohlfarth, B., INTIMATE members, 1998. An event stratigraphy for the Last Termination in the North Atlantic region based on the Greenland ice-core record: a proposal by the INTIMATE group. Journal of Quaternary Science, 13, 4, 283-292.

Brogi, A., 2004. Faults linkage, damage rocks and hydrothermal fluid circulation: Tectonic interpretation of the Rapolano Terme travertines (southern Tuscany, Italy) in the context of Northern Apennines Neogene-Quaternary extension. Eclogae geologicae Helvetiae, 97, 307-320.

Buchenauer, H.W. Gletscher- und Blockgletschergeschichte der westlichen Schobergruppe (Osttirol). Marburger Geographische Schriften, 117, 1-276.

Buczynski, C., and Chafetz, H.S., 1991. Habit of bacterially induced precipitates of calcium carbonate and the influence of medium viscosity on mineralogy. Journal of Sedimentary Petrology, 61, 226-233.

Burns, S.J., Fleitmann, D., Matter, A., Kramers, J. and Al-Subbary, A.A., 2003. Indian Ocean climate and an absolute chronology over Dansgaard/Oeschger events 9 to 13. Science, 301, 1365-1367.

Chafetz, H.S., Patrick, F.R. and Utech, N.M., 1991. Microenvironmental controls on mineralogy and habit of $CaCO_3$ precipitates: an example from an active travertine system. Sedimentology, 38, 107-126.

Chafetz, H.S. and Lawrence, J.R., 1994. Stable isotopic variability within modern travertines. Géographie physique et Quaternaire, 48, 3, 257-273.

Chafetz, H.S. and Guidry, S.A., 2003. Deposition and diagenesis of Mammoth Hot Springs travertine, Yellowstone National Park, Wyoming, U.S.A.. Canadian Journal of Earth Sciences, 40, 1515-1529.

Cheng, H., Edwards, R.L., Hoff, J., Gallup, C.D., Richard, D.A. and Asmerom, Y., 2000. The half-lives of uranium-234 and thorium-230. Chemical Geology, 169, 17-33.

Eikenberg, J., Vezzu, G., Zumsteg, I., Bajo, S., Ruethi, M. and Wyssling, G., 2001. Precise two chronometer dating of Pleistocene travertine: The $^{230}Th/^{234}U$ and $^{226}Ra_{ex}/^{226}Ra(O)$ approach. Quaternary Science Reviews, 20, 1935-1953.

Folk, R.L., Chafetz, H.S. and Tiezzi, P.A., 1985. Bizarre forms of depositional and diagenetic calcite in hot spring travertines, central Italy. In: N. Schneidermann and P.M. Harris (eds.), Carbonate Cements. SEPM Special Publication, 36, 349-369.

Ford, T.D. and Pedley, H.M., 1996. A review of tufa and travertine deposits of the world. Earth-Science Reviews, 41, 117-175.

Fouke, B.W., Farmer, J.D., Des Marais, D.J., Pratt, L., Sturchio, N.C., Burns, P.C. and Discipulo, M.K., 2000. Depositional facies and aqueous-solid geochemistry of travertine-depositing hot springs (Angel Terrace, Mammoth hot springs, Yellowstone National Park; U.S.A.). Journal of Sedimentary Research, 70, 565-585.

Frank, N., Braum, M., Hambach, U., Mangini, A. and Wagner, G., 2000. Warm period growth of travertine during the Last Interglaciation in southern Germany. Quaternary Research, 54, 38-48.

Frisia, S., Borsato, A., Fairchild, I.J., McDermott, F. and Selmo, E.M., 2002. Aragonite-calcite relationships in speleothems (Grotte de Clamouse, France): environment, fabrics and carbonate geochemistry. Journal of Sedimentary Research, 72, 687-699.

Garnett, E.R., Andrews, J.E., Preece, R.C. and Dennis, P.F., 2004a. Climatic change recorded by stable isotopes and trace elements in a British Holocene tufa. Journal of Quaternary Science, 19, 251-262.

Garnett, E.R., Gilmour, M.A., Rowe, P.J., Andrews, J.E. and Preece, R.C., 2004b. $^{230}Th/^{234}U$ dating of Holocene tufas: possibilities and problems. Quaternary Science Reviews, 23, 947-958.

Guo, L. and Riding, R., 1992. Aragonite laminae in hot water travertine crusts, Rapolano Terme, Italy. Sedimentology, 39, 1067-1079.

Harmon, R.S., Glazek, J. and Nowak, K., 1980. $^{230}Th/^{234}U$ dating of travertine from the Bilzingsleben archaeological site. Nature, 284, 132-135.

Hermann, H., 1957. Die Entstehungsgeschichte der postglazialen Kalktuffe der Umgebung von Weilheim (Oberbayern). Neues Jahrbuch für Geologie und Paläontologie Abhandlungen, 105, 11-46.

Huckriede, R., 1975. Ein landschaftsgeschichtlich bedeutsamer Quellkalk im Tiroler Oberinntal. Eiszeitalter und Gegenwart, 26, 181-189.

Ihlenfeld, C., Norman, M.D., Gagan, M.K., Drysdale, R.N., Maas, R. and Webb, J., 2003. Climatic singnificance of seasonal trace element and stable isotope variations in a modern freshwater tufa. Geochimica et Cosmochimica Acta, 67, 2341-2357.

Ivanovich, M. and Harmon, R.S., 1992. Uranium Series Disequilibrium. Applications to Earth, Marine and Environmental Sciences, 2nd edition, Oxford University Press, Oxford, 910 pp.

Jerz, H. and Mangelsdorf, J., 1989. Die interglazialen Kalksinterbildungen bei Hurlach nördlich Landsberg am Lech. Eiszeitalter und Gegenwart, 39, 29-32.

Kano, A., Matsuoka, J., Kojo, T. and Fujii, H., 2003. Origin of annual laminations in tufa deposits, southwest Japan. Palaeogeography, Palaeoclimatology, Palaeoecology, 191, 243-262.

Kim, S.T. and O'Neil, J.R., 1997. Equilibrium and nonequilibrium oxygen isotope effects in synthetic carbonates. Geochimica et Cosmochimica Acta, 61, 3461-3475.

Krois, P., Pavuza, R., Stingl, V. and Turner, H., 1993. Holozäne Wasserfallsinter und Seesedimente bei Hohenberg (Niederösterreich). Geologica et Palaeontologica, 27, 299-300.

Linner, M., 1994. Bericht 1993 über geologische Aufnahmen in der Schobergruppe auf Blatt 179 Lienz. Jahrbuch der Geologischen Bundesanstalt, 137, 517-519.

Linner, M., 1995a. Das ostalpine Kristallin der südwestlichen Schober-Gruppe mit den frühalpidischen Eklogiten im Bereich Prijakte – Alkuser See – Schleinitz. Berichte der Arbeitstagung der Geologischen Bundesanstalt 1995, Vienna, 15-21.

Linner, M., 1995b. Bericht 1994 über geologische Aufnahmen in der südwestlichen Schobergruppe auf Blatt 179 Lienz. Jahrbuch der Geologischen Bundesanstalt, 138, 542-546.

Linner, M., 2003. Bericht 2001 über geologische Aufnahmen in den Deferegger Alpen und in der Granatspitzgruppe auf Blatt 179 Lienz. Jahrbuch der Geologischen Bundesanstalt, 143, 444-453.

Linner, M., 2005. Bericht 2003 über geologische Aufnahmen in den Deferegger Alpen, der Schobergruppe und den Lienzer Dolomiten auf Blatt 179 Lienz. Jahrbuch der Geologischen Bundesanstalt, 145 (in press).

Mallick, R. and Frank, N., 2002. A new technique for precise uranium-series dating of travertine micro-samples. Geochimica et Cosmochimica Acta, 66, 4261-4272.

Mancktelow, N.S., Stöckli, D.F., Grollimund, B., Müller, W., Fügenschuh, B., Viola, G., Seward, D. and Villa, I.M., 2001. The DAV and Periadriatic fault systems in the Eastern Alps south of the Tauern Window. International Journal of Earth Sciences, 90, 593-622.

Matsuoka, J., Kano, A., Oba, T., Watanabe, T., Sakai S. and Seto, K., 2001. Seasonal variation of stable isotopic compositions recorded in a laminated tufa, SW-Japan. Earth and Planetary Science Letters, 191, 31-44.

Merz-Preiß, M. and Riding, R., 1999. Cyanobacterial tufa calcification in two freshwater streams: ambient environment, chemical thresholds and biological processes. Sedimentary Geology, 126, 103-124.

Mix, A.C., Bard, E., Schneider, R., 2001. Environmental processes of the ice age: land, oceans, glaciers (EPILOG). Quaternary Science Reviews, 20, 627-657.

Morse, J.W. and Mackenzie, F.T., 1990. Geochemistry of Sedimentary Carbonates. Elsevier, Amsterdam, 707 pp.

North Greenland Ice Core Project members, 2004. High-resolution record of Northern Hemisphere climate extending into the last interglacial period. Nature, 431, 147-151.

Pazdur, A., Pazdur, M.F., Starkel, L. and Szluc, J., 1988. Stable isotopes of Holocene calcareous tufa in southern Poland as paleoclimatic indicators. Quaternary Research, 30, 177-189.

Pedley, H.M., 1990. Classification and environmental model of cool freshwater tufas. Sedimentary Geology, 68, 143-154.

Pentecost, A., 1995. The Quaternary travertine deposits of Europe and Asia Minor. Quaternary Science Reviews, 14, 1005-1028.

Pentecost, A., 2005. Travertine. Springer, Berlin, 445 pp.

Railsback, L.B., Brook, G.A., Chen, J., Kalin, R. and Fleisher, C.J., 1994. Environmental controls on the petrology of a late Holocene speleothem from Botswana with annual layers of aragonite and calcite. Journal of Sedimentary Research, 64, 147-155.

Reitner, J., Lang, M., Van Husen, D., 1993. Deformation of high slopes in different rocks after Würmian deglaciation in the Gailtal (Austria). Quaternary International, 18, 43-51.

Reitner, J.M., 2000. Large scale toppling and sagging –type deformation in the Schober Group (Eastern Tyrol/Austria): Mechanics, timing and consequences. Terra Nostra, 2000, 91.

Reitner, J.M., 2003. Bericht 1998-1999 über Geologische Aufnahmen im Quartär und Kristallin auf Blatt 179 Lienz. Jahrbuch der Geologischen Bundesanstalt, 143, 514-522.

Reitner, J.M., 2005. Quartärgeologie und Landschaftsentwicklung im Raum Kitzbühel – St. Johann i.T. – Hopfgarten (Nordtirol) vom Riss bis in das Würm-Spätglazial (MIS 6-2). Unpublished PhD thesis, University of Vienna, pp. 190.

Renaut, R.W. and Jones, B., 1997. Controls on aragonite and calcite precipitation in hot spring travertines at Chemurkeu, Lake Bogoria, Kenya. Canadian Journal of Earth Sciences, 34, 801-818.

Romanek, C.S., Grossman, E.L. and Morse, J.W., 1992. Carbon isotopic fractionation in synthetic aragonite and calcite: effects of temperature and precipitation rate. Geochimica et Cosmochimica Acta, 56, 419-430.

Smith, J.R., Giegengack, R. and Schwarcz, H.P., 2004. Constraints on Pleistocene pluvial climates through stable-isotope analysis of fossil-spring tufas and associated gastropods, Kharga Oasis, Egypt. Palaeogeography, Palaeoclimatology, Palaeoecology, 206, 157-175.

Spötl, C., Unterwurzacher, M., Mangini, A. and Longstaffe, F., 2002. Carbonate speleothems and tufas in the dry, inneralpine Vinschgau valley, northernmost Italy: Witnesses of changes in hydrology and climate since the Last Glacial Maximum. Journal of Sedimentary Research, 72, 793-808.

Spötl, C. and Vennemann, T.W., 2003. Continuous-flow isotope ratio mass spectrometric analysis of carbonate minerals. Rapid Communications in Mass Spectrometry, 17, 1004-1006.

Spötl, C., 2005. A robust and fast method of sampling and analysis of $\delta^{13}C$ of dissolved inorganic carbon in ground waters. Isotopes in Environmental and Health Studies, 41, 3, 217-221.

Sturchio, N.C., Pierce, K.L., Murrell, M.T. and Sorey, M.L., 1994. Uranium-series ages of travertines and timing of the last Glaciation in the northern Yellowstone area, Wyoming-Montana. Quaternary Research, 41, 265-277.

Tarutani, T., Clayton, R.N. and Mayeda, T.K., 1969. The effects of polymorphism and magnesium substitution on oxygen isotope fractionation between calcium carbonate and water. Geochimica et Cosmochimica Acta, 33, 986-996.

Troll, G., Forst, R. and Sollner, F., 1976. Uber Bau, Alter und Metamorphose des Altkristallins der Schobergruppe. Osttirol, Geologische Rundschau, 65, 483-511.

Turi, B., 1986. Stable Isotope Geochemistry of Travertines. In: P. Fritz and J.C. Fontes (eds), Handbook of Environmental Isotope Geochemistry. Vol. 2, Elsevier, Amsterdam, pp. 207-238.

Van Husen, D., 2004. Quaternary glaciations in Austria. In: J. Ehlers and P.L. Gibbard (eds.), Quaternary Glaciations - Extent and Chronology. Part I: Europe. Developments in Quaternary Science, 2, p. 1-13, Elsevier, Amsterdam.

Wang, X., Auler, A.S., Edwards, R.L., Cheng, H., Cristalli, P.S., Smart, P.L., Richards, D.A. and Shen, C.C., 2004. Wet periods in northeastern Brazil over the past 210 kyr linked to distant climate anomalies. Nature, 432, 740-743.

Zhou, G.-T. and Zheng, Y.-F., 2003. An experimental study of oxygen isotope fractionation between inorganically precipitated aragonite and water at low temperatures. Geochimica et Cosmochimica Acta, 67, 387-399.

Zötl, J., Goldbrunner, J.E., 1993. Die Mineral- und Heilwässer Österreichs. Geologische Grundlagen und Spurenelemente. Springer, Vienna, 324 pp.

Received: 10. September 2005
Accepted: 28. November 2005

Ronny BOCH[1)*], Christoph SPÖTL[1)], Jürgen M. REITNER[2)] & Jan KRAMERS[3)]

[1)] Institut für Geologie und Paläontologie, Leopold-Franzens-Universität Innsbruck, Innrain 52, 6020 Innsbruck, Austria

[2)] Geologische Bundesanstalt, Neulinggasse 38, 1030 Wien, Austria

[3)] Institut für Geologie, Universität Bern, Erlachstraße 9a, 3012 Bern, Switzerland

[*)] Corresponding author: Ronny Boch (ronny.boch@uibk.ac.at)